Terrace selection during equilibration at an icosahedral quasicrystal surface

B. Unal, T. A. Lograsso, A. Ross, C. J. Jenks, and P. A. Thiel*
Departments of Materials Science & Engineering and of Chemistry, and the Ames Laboratory, Iowa State University, Ames, Iowa 50011, USA

(Received 18 October 2004; revised manuscript received 4 January 2005; published 8 April 2005)

We investigate the equilibration of a fivefold surface of the icosahedral Al-Pd-Mn quasicrystal at 900–915 and 925–950 K, using scanning tunneling microscopy. After annealing at the lower temperatures, there is a high density of shallow voids on some terraces but not on others; at 925–950 K, the void-rich terraces are much rarer. The terminations that are consumed by voids exhibit a distinctive local atomic configuration, called a "ring" by previous authors. Apparently, through growth and coalescence of the voids, a different termination becomes exposed on the host terraces, which also leads to a change in step heights at the edges of the terraces. We suggest that the shallow steps associated with the voids, and the ring configuration, signal a surface that is in an intermediate stage of structural equilibration.

DOI: 10.1103/PhysRevB.71.165411 PACS number(s): 68.35.−p, 61.44.Br, 68.47.De

I. INTRODUCTION

Quasicrystals are *nonperiodic*, yet well-ordered, intermetallics. Most known quasicrystals are icosahedral, and most contain 60–70 at. % of aluminum. Studies of their surfaces are motivated by the fact that the icosahedral, aluminum-rich alloys exhibit unusual surface properties, including low adhesion to polar liquids and low friction.[1–3]

Clean surfaces of quasicrystals have been studied intensely, and some general principles have emerged. First, a rich diversity of structures can form, depending upon the history of sample treatment and the length scale of the structural examination. This array of surface morphologies includes rough surfaces,[4–9] faceted voids,[10] and smooth (to within a few tenths of an angstrom) terraces.[6,8,9,11–16] The latter type of structure—flat terraces—is the topic of this paper.

Second, the terraces typically exhibit a fine structure, probed by scanning tunneling microscopy (STM), which is consistent with bulk models of quasicrystalline structure.[13,15–17] This indicates that the lateral (in-plane) atomic structure is bulk terminated, resolving a previous controversy over whether bulk termination of a quasicrystal was compatible with a flat surface.

Third, in the bulk-terminated quasicrystal surface, only a subset of all possible bulk planes corresponds to surface terminations. The surface terminations are believed to actually be pairs of planes, separated by 0.48 Å in the bulk, but contracted at the surface to 0.38–0.42 Å. These two planes have a combined density comparable to that of the close-packed surface of pure Al and a combined composition higher in Al than the bulk average.[14,18–23]

Fourth, the quasicrystalline terraces are separated by steps whose heights are not integral multiples, but rather successive multiples of τ, the golden mean $(\tau = 2\cos(\pi/5) = (1+\sqrt{5})/2 = 1.618\ldots)$. Reports of the step height values have ranged from 6.2 to 6.8 Å for the longest (L), 4.0 to 4.2 Å for the medium step (M), and 2.4 to 2.6 Å for the shortest (S), with uncertainties of about ±0.2 Å. (In some other papers, these three steps have been named L, S, and S/τ, respectively.) Here, we are not so concerned with the actual step height values as with their frequencies of occurrence. Previous reports have been inconsistent. One study reported *only* L and M, arranged in a Fibonacci sequence, which implies a relative abundance of $L/M = \tau$.[11] In contrast, another paper noted that the L and S steps were common, and the M steps were rare.[12] A quantitative analysis in yet another paper indicated that the relative abundance decreased from L to M to S, with frequency ratios $L/M \approx M/S \approx \tau$.[14]

Fifth, the method used to produce the bulk-terminated terraces involves massive changes in both surface composition and surface structure. Ion bombardment at room temperature produces an Al-deficient phase. Annealing between 300 and 700 K yields a very rough crystalline surface phase (lacking discernible terraces) that is relatively Al deficient. There is evidence that migration of bulk vacancies to the surface contributes to this roughness.[10] At higher temperatures, the surface usually changes to a flat quasicrystalline phase.[24] An intermediate phase that is both quasicrystalline and rough may form around 700 K.[8] Flat *crystalline* phases can also form above 700 K.[25–29] The factors that select between crystalline and quasicrystalline surface phases above 700 K are poorly understood.

In this paper, we show that equilibration during annealing is a more complex and subtle process than previously thought. Even after the quasicrystalline terrace-step structure appears, it evolves with time and temperature. There is a selection among possible terminations, during which some terraces disappear, while other (slightly different) types of terraces survive. This evolution also affects the step heights and may explain previous discrepancies in the literature.

II. EXPERIMENTAL DESCRIPTION

A single grain of icosahedral Al-Pd-Mn was grown by the Bridgman method. Its bulk composition was $Al_{70.2}Pd_{20.7}Mn_{9.1}$, based on scanning electron microscopy and energy dispersive spectroscopy. The grain was sliced

perpendicular to its fivefold axis and polished to a mirror finish, using 6-, 1-, and 0.25-μm diamond paste on Texmet cloth. The resultant sample was a flat wafer with an area of 6×5 mm^2 and thickness of 1.5 mm, identification No. ARR-4-12-2.1.

The wafer was then mounted on a Ta plate and put into an ultrahigh-vacuum (UHV) chamber equipped for low-energy electron diffraction (LEED), Auger electron spectroscopy (AES), STM, ion bombardment, mass spectrometry, and sample heating. A clean surface was gained after cycles of Ar^+ sputtering at room temperature (RT) for 30 min and annealing at 900 K for 3 h. The Ar^+ ion energy was reduced from 2 to 1 keV by 0.5-keV increments in the first two cycles and kept constant at 1 keV during the rest of the etching process. The total times for sputtering and annealing were 3 and 18 h, respectively. A sharp LEED pattern was achieved after this cleaning process.

After its initial cleaning, the sample was used for other types of experiments. Consequently, it underwent 26 sputter-anneal cycles and about 60 cumulative hours of annealing at 950 K in UHV. At that point, the experiments described in this paper began. Several observations were made after 950 K anneals. The annealing temperature was then successively lowered to the 900–915 K range, while several more observations were recorded. After this, the sample was removed, repolished, and recleaned in UHV, and more experiments were done in the 900–915 K range. The data reported herein were reproducible and consistent throughout.

Before each individual STM experiment, we sputtered the sample with Ar^+ at 1 keV (2.4 μA sample to ground with +20 V bias) for 30 min and then annealed it for 3 h at a specified temperature in the range 900–950 K, by changing the power of the heating element. After annealing, the sample was cooled slowly to RT. The cooling rate from the annealing temperature to 700 K was controlled at about 12.5 K/min. Before annealing, the surface cleanliness was verified by AES. All the STM images were taken at RT with tunneling conditions of +0.97 V and 0.47 nA. The typical base pressure during an STM measurement was below 4×10^{-11} Torr.

Temperature was monitored using an infrared pyrometer with emissivity set at 0.35.[25] Sources of error in the measurement include film deposition on the window used for pyrometry (due to evaporation from the sample and other sources), stray radiation from the filament heater, and thermal gradients across the (poorly conductive) sample. Based upon comparisons with two sets of K-type thermocouples located at different spots on the sample holder and upon pyrometer readings taken from different points on the sample itself, we estimate that the accuracy in sample temperatures reported here is about ±25 K, and this should be kept in mind when comparing temperatures reported by other laboratories. Reproducibility is better, although it still is affected by thermal gradients within the sample and hence by the region chosen for imaging.

III. EXPERIMENTAL RESULTS AND INTERPRETATION

Figure 1(a) shows a large-scale STM image—5000 Å $\times$5000 Å—of a 5*f* Al-Pd-Mn surface, after annealing at 900 K for 3 h. It is clear that there are two types of terraces. One type has many pockets, or voids, and hence has a mottled appearance. The other type is smooth and nearly void free. Figures 1(b) and 1(c) also illustrate the existence of these two types of terraces, after annealing at 915 K for 3 h.

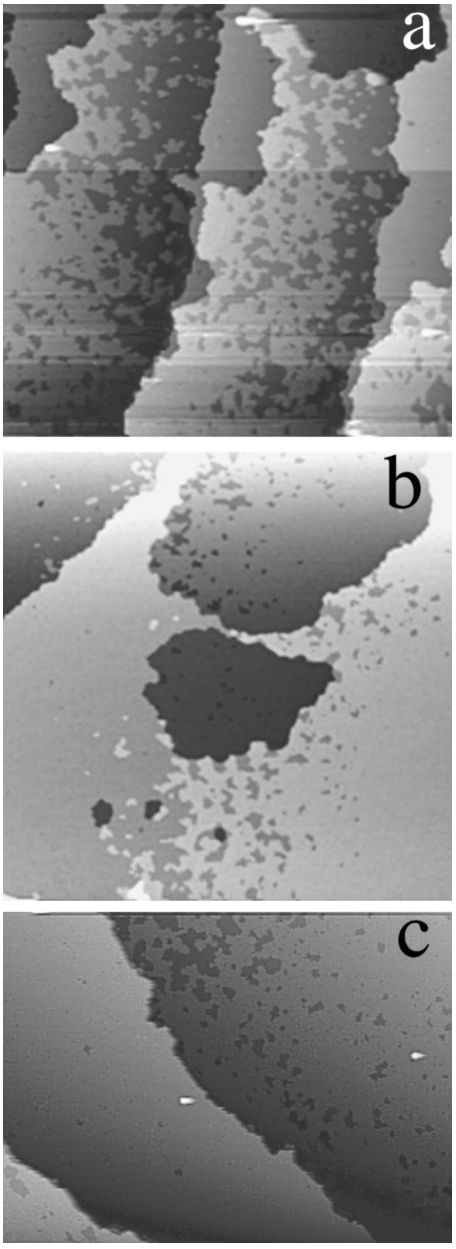

FIG. 1. STM images of 5*f* *i*-Al-Pd-Mn, illustrating the existence of void-rich and nearly-void-free terraces. (a) 5000 Å $\times$5000 Å, after annealing at 900 K. (b) 5000 Å$\times$5000 Å, after annealing at 915 K. (c) 500$\times$365 Å, after annealing at 915 K.

The steps in Fig. 1 fall into the three known groups identified in Sec. I as *L*, *M*, and *S*. Almost all of the voids on the mottled terraces are bordered by *S* steps.

Figure 2(a) is a 1000 Å$\times$1000 Å image from a surface prepared in a different experiment, but under nominally identical conditions. Four layers are visible and are labeled 1–4, with layer 1 being topmost. Figure 2(a) is essentially an im-

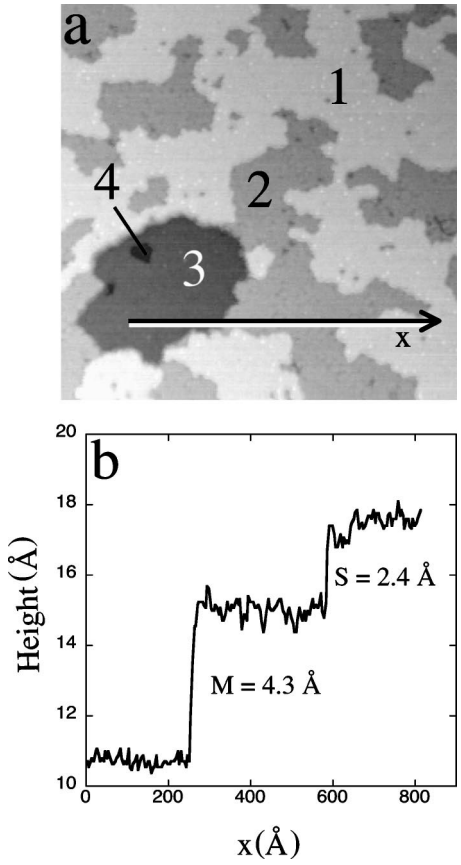

FIG. 2. (a) 1000 Å×1000 Å STM images of the 5*f* Al-Pd-Mn surface after annealing at 900 K. (b) Line profile across (a). For step-height evaluation, see text.

age of a very large, mottled terrace, in which about half of layer 1 has been removed and half of layer 2 has been exposed. In a localized region of Fig. 2(a), deeper layers—3 and 4—are also visible. Figure 2(b) is a line profile across the arrow in Fig. 2(a). This shows that layers 1 and 2 are separated by *S* steps, whereas layers 2 and 3 are separated by an *M* step.

As an aside, note that the height values that we report for the *L*, *M*, and *S* steps, such as the values given in Fig. 2(b), are not extracted from line profiles, since we find that such values are unreliable. Presumably, this is due to short-scale roughness on the terraces, and longer-range curvature sometimes occurring near the step edges. Both effects are visible in Fig. 2(b). Instead, step height values are much more precise if they are extracted from a histogram of pixel heights in a *rectangular area* that encompasses the step and adjoining terraces, a procedure developed originally by Cai *et al.*[14]

Figure 3 reveals regions of this same surface at higher resolution. Panels (a), (b), and (c) are taken from layers 1, 2, and 3, respectively. A number of local motifs, previously identified in other work,[16] can be seen in each of the three layers. Following previous nomenclature,[16] these are labelled as white stars, dark stars, and white flowers. In Figs. 3(a) and 3(c) (layers 1 and 3), certain additional local configurations look like rings. Rings cannot be found on layer 2 [panel (b)]. Therefore, we postulate that the mottled terraces belong to the class of surfaces that include the "ring" planes in previous work by Papadopolos *et al.*[16] and that the nearly-void-free terraces belong to the class of surfaces that include the "clear" planes and "Schaub" planes.[16]

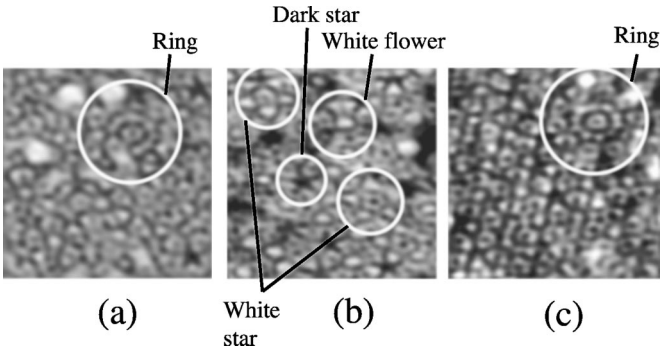

FIG. 3. Magnified regions of the three layers labeled in Fig. 2. All images have been filtered. White circles and labels point out local features identified in Ref. 16. (a) 77×77 Å STM image of layer No. 1 in Fig. 2(a). (b) 77×77 Å STM image of layer No. 2 in Fig. 2(a). (c) 77×77 Å STM image of layer No. 3 in Fig. 2(a).

Figure 4(a) shows the terrace structure that results after annealing at 925 K. Three points are noteworthy. First, at this higher temperature, the mottled terraces are much less frequent, and the surviving terraces are generally larger. Second, a number of small islands are visible on the middle terrace, particularly within the oval. These small islands are 2.5 Å high and are probably remnants of a void-rich termi-

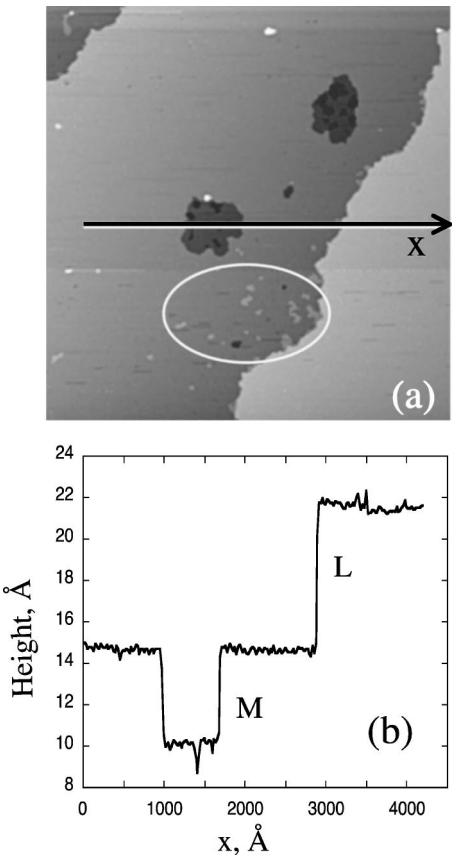

FIG. 4. (a) 5000 Å×5000 Å STM image after annealing at 925 K. (b) Line profile as indicated by the arrow in (a).

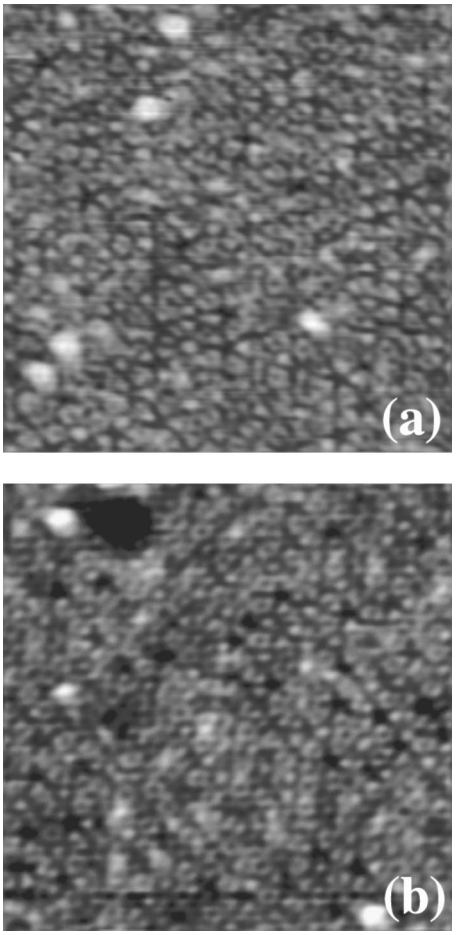

FIG. 5. High-resolution views of two void-poor terraces, like those shown in Fig. 4(a). The images are both 150 Å × 150 Å in size and have been filtered.

nation that was present at an earlier stage. In other words, this entire terrace was probably 2.5 Å higher, earlier in its evolution. Third, pits are visible on the middle terrace, but they are different than the voids on the mottled terraces represented in Fig. 1, because these depressions are circumscribed by *M*-type steps. Deeper levels—about 2.5 Å lower—are also becoming exposed at the bottoms of the pits. These aspects of the pits are illustrated by the line profile in Fig. 4(b). The sharp dip at $x \approx 1400$ Å corresponds to a void at the bottom of the larger pit; its depth and shape, however, are not resolved completely because it is small relative to the size of the image. Apparently, void-rich terminations comprise the floors of these *M*-type pits.

The fine structure on relatively smooth terraces, such as those in Fig. 4(a), is illustrated in Figs. 5(a) and 5(b). No rings can be found. Hence, annealing to higher temperature significantly reduces the occurrence of the terminations that contain ring configurations.

Upon heating to 950 K, the data are very similar to those at 925 K. Some void-rich terraces can still be found, but they are significantly less abundant than at the lower range of annealing temperature, 900–915 K.

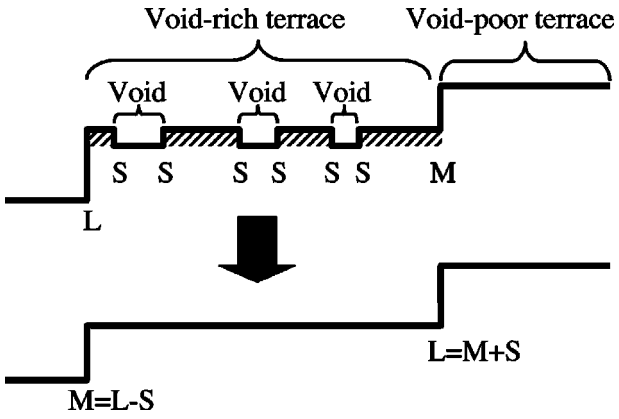

FIG. 6. Schematic depiction of the proposed model for terrace selection at 900–915 K.

IV. DISCUSSION

Our main postulate is that, by annealing to 900–915 K and 925–950 K, we are capturing the surface in two different stages of evolution.

First, consider the 900–915 K surface. The data (e.g., Fig. 1) show that the voids are bordered by *S* steps. This means that the surface must evolve as illustrated in Fig. 6, which is a schematic cross section of the surface. Loss of material from the crosshatched regions first creates the voids and gives the terrace a mottled appearance. The growth of the voids increasingly exposes a lower termination. When the voids have completely overtaken the terrace, its level is lowered by the step height of the voids, *S*. Hence, the lowering of the terrace changes the down-going step (the one in the left side of Fig. 6) from *L* to $L-S=M$, and the up-going step (in the right side) from *M* to $M+S=L$. The step heights *L* and *M* are chosen arbitrarily for illustration.

The atomic nature of the void-rich versus (nearly) void-free terminations can be identified on the basis of local configurations in the STM images. The critical difference is that the void-rich terminations display the ring configuration, while the others do not.

Papadopolos *et al.*[16] related STM images to specific types of terminations in their three-dimensional tiling model of bulk structure. Within the context of that model and in agreement with experimental work from many groups (as reviewed in Sec. I), all terminations consist of pairs of planes separated (in the bulk) by 0.48 Å. Furthermore, the combined density of these two planes is constant.

In the work of Papadopolos *et al.*[16] two different types of terminations could be identified in the STM data, based on different local configurations. They interpreted these as terminations with different relative densities in the top and underlying plane (the *q* and *b* plane, respectively, in their nomenclature). In the termination where the density of the top plane is less than the density of the second, the rings shown in Figs. 3(a) and 3(c) were predicted and observed. In the termination where the densities were reversed, no rings were observed and the planes were called "clear." The combined densities of the two planes was effectively constant.

The relative densities could provide a rationale for a slightly lower stability of terminations containing the ring

FIG. 7. Schematic depiction of the proposed model for evolution of long-range surface morphology at 700–950 K.

configuration, since higher density is known to be associated with lower surface energy—in elemental metals.[30–32] It has been proposed that this rule also applies to quasicrystals.[22] Since the termination containing rings has a higher atomic density in the very outermost plane, it would have a lower stability. Differences in chemical composition could also contribute to different stabilities of different terminations.

Two detailed structural analyses of this system have been carried out, using two different techniques (low-energy electron diffraction and x-ray photoelectron diffraction) but both based upon electron scattering.[18,19,23] Both analyses found that a certain group of terminations gave the best agreement with experiment, but another group of terminations gave moderately good agreement with experiment. This second group included terminations in which the outermost plane had a lower density than the underlying plane, analogous to the ring-plane terminations of Papadopolos *et al.*[16] The electron scattering analyses left open the possibility that this second group made a minor contribution to the experimental electron scattering data and hence made a minor contribution to the total surface area, in accordance with our model.

Consider the sequence of morphological changes that the surface undergoes. This sequence is illustrated schematically in Fig. 7. Starting from a rough surface without discernible terraces, extensive mass transport allows terraces to emerge between 700 and 900 K. Apparently, there are kinetic limitations in this stage that lead to different types of terraces with different stabilities. At 900 K, new processes begin which lead to selection among the terrace terminations. There are two possibilities for these new processes.

The first is evaporation into the gas phase. Schmithüsen *et al.*[26] reported that evaporation of Mn begins at 900 K and of Al at 1000 K, this order corresponding to the order of the elemental vapor pressures. Hence, evaporation at these temperatures is nonstoichiometric. The irreversible loss of Mn at 900 K could trigger rearrangements on the terraces that lead to the voids. At 900 K, the remaining Al and Pd could diffuse away to segregate at step edges or defect sites, or to form crystalline surface phases.

The second possibility is that new diffusion processes become activated at 900 K. However, mass transport is already extensive below 900 K—so extensive that the terraces form. For example, the root-mean-square displacement of a bulk Mn atom (the slowest diffuser in this alloy) is 25 and 50 μm, at temperatures of 900 and 950 K, over 3 h.[33] The fact that this displacement is very large and differs only by a factor of 2 over the temperature range 900–950 K supports the hypothesis that mass transport is extensive already at or below 900 K and does not change dramatically between 900 and 950 K. It has been suggested that surface modification due to migration of bulk defect vacancies also begins in a significantly lower temperature range.[10] Hence, it seems unlikely that new diffusion processes begin around 900 K.

An entirely different interpretation might be that the void-rich terraces do not reflect the relative stability of different terminations, but rather are the result of vacancies migrating from the bulk to the surface and condensing there.[10,34,35] Indeed, there is evidence that this type of diffusion eventually produces a vacancy-depleted near-surface region that is a few microns deep.[34] In that case, one would expect the void-rich terraces to occur early in the life of the sample and to disappear over time. However, this is the opposite of the sequence of our experiments, wherein most of the higher-temperature observations of void-free terraces preceded the lower-temperature observations of void-rich terraces. See Sec. II. Furthermore, in order to account for our observations, the bulk vacancies would have to accumulate preferentially on specific terraces. Taken together, these facts make the vacancy condensation hypothesis seem unlikely.

It is commonly accepted that the "best" surfaces on *i*-Al-Pd-Mn, for purposes of STM work, are produced by annealing at 950–975 K or even higher. This falls above the temperature range where the voids are most abundant, 900–915 K. (There may be some small overlap when the probable uncertainty of ±25 K, described in Sec. II, is taken into account and applied both to our own temperatures and to those from other laboratories.) Hence, one would expect that the void-rich terraces are rather rare on the "best" surfaces. Perhaps this is why the evolution of terrace structure has gone unnoticed until now. It is interesting to note that some narrow, void-rich terraces are discernible in STM data published by Ledieu *et al.*, notably Fig. 1 of Ref. 22.

V. CONCLUSION

The terraced, bulk-terminated quasicrystal undergoes equilibration at 900–950 K, in which certain terraces are modified by the growth and coalescence of voids. This process leads to a change in step heights, particularly a reduction in the density of the *S* steps. The process also leads to a reduction of the terminations that exhibit local ring configurations. We postulate that both the *S* steps and the local ring configurations occur on terminations that are higher in energy than the others (metastable). A new process—one that was not operative during initial terrace formation—takes effect at and above 900 K. This process, which may be evaporation into the gas phase, facilitates selection among different terminations.

The ring terminations may be less stable because of subtle differences in the densities of the top two planes. Specifically, in the ring terminations the outermost plane is less dense than the (very-close) second plane. In the other terminations, the densities of these two planes are reversed. The combined density of the two planes is nearly constant. A minor contribution from terminations with relative densities corresponding to the ring termination would be consistent with previous structural analyses that were based upon dynamical electron scattering.

ACKNOWLEDGMENTS

We thank Zorka Papadopolos for many helpful discussions. This work was supported by the Director, Office of Science, Office of Basic Energy Science, Materials Science Division of the U.S. Department of Energy under Contract No. W-405-Eng-82.

*Corresponding author. Electronic address: thiel@ameslab.gov

[1] J. M. Dubois, P. Brunet, W. Costin, and A. Merstallinger, J. Non-Cryst. Solids **334-335**, 475 (2004).
[2] J. M. Dubois, J. Non-Cryst. Solids **334-335**, 481 (2004).
[3] J. M. Dubois, V. Fournée, and E. Belin-Ferré, in *Quasicrystals 2003—Preparation, Properties and Applications*, edited by E. Belin-Ferré, M. Feuerbacher, Y. Ishii, and D. J. Sordelet, MRS Symposia Proceedings, No. 805 (Materials Research Society, Warrendale, PA, 2004), p. 287.
[4] P. Ebert, M. Feuerbacher, N. Tamura, M. Wollgarten, and K. Urban, Phys. Rev. Lett. **77**, 3827 (1996).
[5] P. Ebert, F. Yue, and K. Urban, Phys. Rev. B **57**, 2821 (1998).
[6] G. Cappello, F. Schmithüsen, J. Chevrier, F. Cominb, A. Stierle, V. Formoso, M. de Boissieu, M. Boudard, T. A. Lograsso, C. Jenks, and D. Delaney, Mater. Sci. Eng., A **294-296**, 822 (2000).
[7] P. Ebert, F. Kluge, B. Grushko, and K. Urban, Phys. Rev. B **60**, 874 (1999).
[8] J. Ledieu, A. Munz, T. Parker, R. McGrath, R. D. Diehl, D. W. Delaney, and T. A. Lograsso, Surf. Sci. **433-435**, 666 (1999).
[9] G. Cappello, J. Chevrier, F. Schmithüsen, A. Stierle, V. Formoso, F. Comin, M. de Boissieu, M. Boudard, T. Lograsso, C. Jenks, and D. Delaney, Phys. Rev. B **65**, 245405 (2002).
[10] P. Ebert, M. Yurechko, F. Kluge, T. Cai, B. Grushko, P. A. Thiel, and K. Urban, Phys. Rev. B **67**, 024208 (2003).
[11] T. M. Schaub, D. E. Bürgler, H.-J. Güntherodt, and J. B. Suck, Phys. Rev. Lett. **73**, 1255 (1994).
[12] Z. Shen, C. Stoldt, C. Jenks, T. Lograsso, and P. A. Thiel, Phys. Rev. B **60**, 14 688 (1999).
[13] J. Ledieu, R. McGrath, R. D. Diehl, T. A. Lograsso, D. W. Delaney, Z. Papadopolos, and G. Kasner, Surf. Sci. **492**, L729 (2001).
[14] T. Cai, F. Shi, Z. Shen, M. Gierer, A. I. Goldman, M. J. Kramer, C. J. Jenks, T. A. Lograsso, D. W. Delaney, P. A. Thiel, and M. A. Van Hove, Surf. Sci. **495**, 19 (2001).
[15] T. Cai, V. Fournée, T. Lograsso, A. R. Ross, and P. A. Thiel, Phys. Rev. B **65**, 140202(R) (2002).
[16] Z. Papadopolos, G. Kasner, J. Ledieu, E. J. Cox, N. V. Richardson, Q. Chen, R. D. Diehl, T. A. Lograsso, A. R. Ross, and R. McGrath, Phys. Rev. B **66**, 184207 (2002).
[17] L. Barbier, D. Le Floc'h, Y. Calvayrac, and D. Gratias, Phys. Rev. Lett. **88**, 085506 (2002).
[18] M. Gierer, M. A. Van Hove, A. I. Goldman, Z. Shen, S.-L. Chang, C. J. Jenks, C.-M. Zhang, and P. A. Thiel, Phys. Rev. Lett. **78**, 467 (1997).
[19] M. Gierer, M. A. Van Hove, A. I. Goldman, Z. Shen, S.-L. Chang, P. J. Pinhero, C. J. Jenks, J. W. Anderegg, C.-M. Zhang, and P. A. Thiel, Phys. Rev. B **57**, 7628 (1998).
[20] M. J. Capitan, J. Alvarez, J. L. Joulaud, and Y. Calvayrac, Surf. Sci. **423**, L251 (1999).
[21] C. Jenks, A. Ross, T. A. Lograsso, J. A. Whaley, and R. Bastasz, Surf. Sci. **521**, 34 (2002).
[22] Z. Papadopolos, P. Pleasants, G. Kasner, V. Fournée, C. J. Jenks, J. Ledieu, and R. McGrath, Phys. Rev. B **69**, 224201 (2004).
[23] J.-C. Zheng, C. H. A. Huan, A. T. S. Wee, M. A. Van Hove, C. S. Fadley, F. J. Shi, E. Rotenberg, S. R. Barman, J. J. Paggel, K. Horn, P. Ebert, and K. Urban, Phys. Rev. B **69**, 134107 (2004).
[24] Z. Shen, M. J. Kramer, C. J. Jenks, A. I. Goldman, T. A. Lograsso, D. W. Delaney, M. Heinzig, W. Raberg, and P. A. Thiel, Phys. Rev. B **58**, 9961 (1998).
[25] J. Ledieu, C. A. Muryn, G. Thornton, G. Cappello, J. Chevrier, R. D. Diehl, T. A. Lograsso, D. Delaney, and R. McGrath, Mater. Sci. Eng., A **294-296**, 871 (2000).
[26] F. Schmithüsen, G. Cappello, M. D. Boissieu, M. Boudard, F. Comin, and J. Chevrier, Surf. Sci. **444**, 113 (2000).
[27] D. Naumovic, P. Aebi, L. Schlapbach, C. Beeli, K. Kunze, T. A. Lograsso, and D. W. Delaney, Phys. Rev. Lett. **87**, 195506 (2001).
[28] C. J. Jenks, T. E. Bloomer, M. J. Kramer, T. A. Lograsso, D. W. Delaney, A. R. Ross, D. J. Sordelet, M. F. Besser, and P. A. Thiel, Appl. Surf. Sci. **180**, 57 (2001).
[29] V. Fournée, A. R. Ross, T. A. Lograsso, J. W. Anderegg, C. Dong, M. Kramer, I. R. Fisher, P. C. Canfield, and P. A. Thiel, Phys. Rev. B **66**, 165423 (2002).
[30] H. L. Skriver, and N. M. Rosengaard, Phys. Rev. B **46**, 7157 (1992).
[31] M. J. Mehl, and D. A. Papaconstantopoulos, Phys. Rev. B **54**, 4519 (1996).
[32] L. Vitos, A. V. Ruban, H. L. Skriver, and J. Kollár, Surf. Sci. **411**, 186 (1998).
[33] W. Sprengel, T. A. Lograsso, and H. Nakajima, Phys. Rev. Lett. **77**, 5233 (1996).
[34] F. Schmithüsen, Ph.D. thesis, Université J. Fourier, 2001.
[35] S. Agliozzo, J. Gastaldi, H. Klein, J. Härtwig, J. Baruchel, and E. Brunello, Phys. Rev. B **69**, 144204 (2004).